Proceedings of ICONE 8
8th International Conference on Nuclear Engineering
April 2-6, 2000, Baltimore, MD USA

ICONE-8320

STUDY OF ALLOYING ELEMENTS IN THE ZR MATRIX OF ZIRCALOY-4 AND ZIRLO USING THE ADVANCED PHOTON SOURCE AT ARGONNE.

O. Delaire
Department of Mechanical and Nuclear Engineering, The Pennsylvania State University
231 Sackett Building
University Park, PA 16802 US
(814) 863-3644
(814) 865-8499
oxd110@psu.edu

K. T. Erwin
Department of Mechanical and Nuclear Engineering, The Pennsylvania State University
231 Sackett Building
University Park, PA 16802 US
(814) 863-3644
(814) 865-8499
kte102@psu.edu

A. T. Motta
Department of Mechanical and Nuclear Engineering, The Pennsylvania State University
231 Sackett Building
University Park, PA 16802 US
(814) 865-0036
(814) 865-8499
atm2@psu.edu

R. C. Birtcher
Materials Science Division,
Argonne National Laboratory,
MSD 212 E203
9700 South Cass Ave
Argonne, IL 60439 US
(630) 252-4996
(630) 252-4289
birtcher@anl.gov

J. M. Maser
Advanced Photon Source,
Argonne National Laboratory,
XFD 401 B3181
9700 South Cass Ave.
Argonne, IL 60439 US
(630)-252-1081
(630)-252-9303
maser@aps.anl.gov

B. Lai
Advanced Photon Source,
Argonne National Laboratory,
XFD 401 B3194
9700 South Cass Ave.
Argonne, IL 60439 US
(630)-252-6405
(630)-252-9303
blai@aps.anl.gov

KEY WORDS Zirconium alloys, Zircaloy, alloying elements, synchrotron radiation, x-ray fluorescence.

ABSTRACT

The alloying element content present in the α-Zr matrix of Zr alloys, especially the concentration and distribution of the transition elements Fe, Cr, Ni is crucial to determining the alloy corrosion behavior. However, the levels of these elements in the Zr matrix are so low that they cannot be measured by traditional techniques. Using the unique combination of spatial and elemental resolution achieved in the microbeam line at the Advanced Photon Source at Argonne (APS), we can study the alloying element concentration in the hexagonal matrix of α-Zr with a precision hitherto not achieved. In this research program we use x-ray fluorescence from a sub-micron x-ray beam to study these alloying element concentration in the matrix as a function of alloy type, thermo-mechanical treatment and irradiation conditions. The information thus obtained will allow more precise and mechanistic predictions of alloy behavior, especially in conditions of high fuel burnup. In this preliminary study, we report on the initial determinations of matrix alloying element concentrations for standard non-irradiated alloys, both in the quenched and annealed states.

The results from 2D-fluorescence scans clearly show that we can spatially distinguish the precipitates from the matrix using the fluorescence signal. We found that significantly sharper ratios of concentrations can be obtained from thin foil samples than from dimpled or bulk samples, indicating that the influence of buried layers is significant. We examined the difference between alloying contents of quenched samples of the different alloys, using TEM samples. The values we obtained were in good agreement with the nominal values for Zircaloy-4 and with the measured values for ZIRLO. We also briefly examined the alloying content in the matrix of as-fabricated Zircaloy-4 and found it to be higher than estimated

by others, likely as a result of a beam size that was larger than expected. We examine these results and present our future research plans, which include performing similar examinations on neutron-irradiated samples.

INTRODUCTION

Zircaloy-4 and ZIRLO are used for fuel cladding tubes and core structural materials in water-cooled nuclear reactors. The microstructure of these alloys, and especially the distribution of alloying elements, strongly influences their behavior under neutron irradiation, especially at high fuel burnup [1]. Both of these alloys are Zr-based; Zircaloy-4 contains approximately 98% Zr, 1.4% Sn, and a total of 0.4% of Fe and Cr; ZIRLO is composed of 1.2% Nb, 0.1% Fe, 1% Sn and balance Zr [1], (table 1). Sn is found in solid solution in the matrix while Fe, Cr and Nb mostly form intermetallic precipitates because of their very low solubility in α-Zr, which is the stable phase at both reactor and room temperature (the temperature of eutectoid decomposition of β-Zr is 820ºC). Borrelly [2], Zou [3] and Charquet [4] have determined solubility limits for Fe in Zr at 800ºC of about 110 wt. ppm (equivalent to 0.011 wt. %), using different techniques. Charquet et. al. quote a solubility limit at 810ºC for (Fe+Cr) with Fe/Cr=2 in Zr-1.4%Sn-0.1%O of 150 wt. ppm (equivalent to 0.015 wt. %) [4]. Those solubility limits are even lower at room temperature, estimated on the order of several parts per million in pure Zr.

The transition elements in solid solution in α-Zr are suspected to influence corrosion resistance in these alloys, as well as the kinetics of irradiation growth. Irradiation growth can become limiting in some reactor designs, especially if breakaway growth occurs through the formation of <c> component dislocations. The reason for the occurrence of the <c>-component dislocations after a fluence of 3×10^{25} $n.m^{-2}$ (as well as their impact on growth) is still an open question, but the contribution of minor alloying elements in stabilizing those dislocations is suspected [8]. Uniform corrosion is a limiting phenomenon in PWRs, especially for high burnup fuel. Although a general scheme of the phase transformation in the zirconia is available, the details of the corrosion mechanism are still to be described accurately. In particular, the effect of alloying elements and their distribution in the Zr matrix is of importance [5]. The size and distribution of second phase particles is also a factor in determining corrosion resistance, therefore the partition of alloying elements between the precipitates and the matrix is of interest. The alloying elements in solution can undergo irradiation-induced precipitation, and the precipitates can become amorphous and dissolve when exposed to the fast neutron flux [6,7]. Iron is one of the primary alloying elements in Zircaloy-4 and ZIRLO, and appears to influence high temperature mass transport [8] as well as irradiation damage [9] and corrosion [10,11]. Because of this it is important to determine accurately the concentration of trace alloying elements such as Fe in the Zr matrix. For the first time, the combination of elemental and spatial resolution necessary to do so is available at the Advanced Photon Source facility at Argonne National Laboratory (ANL).. We present here some initial measurements of Fe content in the Zr matrix of Zircaloy 4 and ZIRLO and discuss the advantages of microscopic x-ray fluorescence combined with synchrotron radiation.

NOMENCLATURE

A: x-ray beam cross-sectional area
N: precipitate number density
SR: synchrotron radiation.
ZL: ZIRLO
Z4: Zircaloy-4
l: average inter-precipitate distance
w: sample thickness
μ-XRF: microscopic x-ray fluorescence

	Zircaloy-4 (weight %)	ZIRLO (weight %)
Fe	0.24	0.11
Cr	0.11	0.001
Sn	1.64	1.08
Ni	0.0034	<0.001
Nb	-	1.23
O	0.112	0.145
N	0.002	0.005
C	0.003	0.002
Si	0.0095	0.013
Cu	0.002	0.002
Hf	<0.004	<0.004
Al	0.0058	0.012
Mn	<0.001	<0.001
Mo	<0.001	<0.001
Ti	0.0012	0.0019
W	<0.004	<0.004

Table 1 Measured composition for Zircaloy-4 and ZIRLO.

1 EXPERIMENTAL METHODS

Numerous techniques are available to analyze compositions of samples or obtain spatial distribution of elements, but very few allow the quantitative determination of the concentration of a trace element on a microscopic basis. For example, the conventional energy dispersive spectrometry (EDS) used in transmission electron microscopes (TEM)

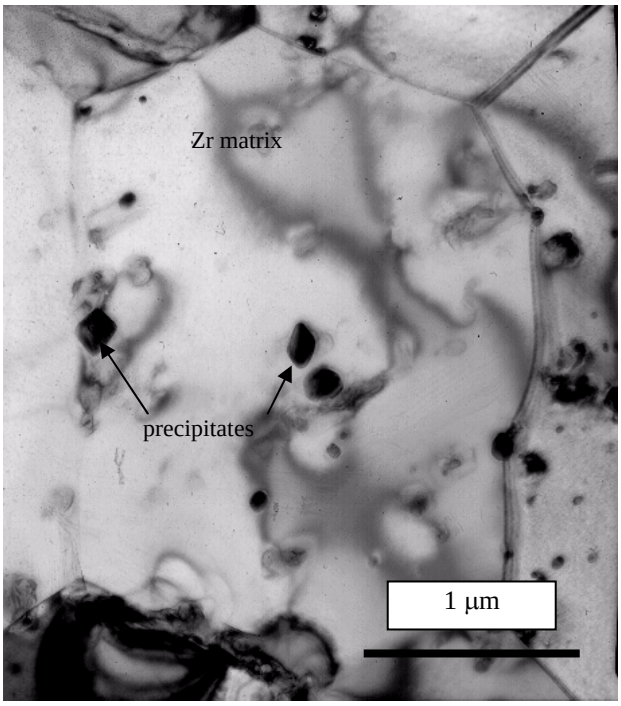

Fig. 1: Bright Field TEM micrograph from recrystallized Zircaloy-4.

proves unable to detect the analytes of interest at the very low levels found in our materials. Microscopic x-ray fluorescence (μ-XRF) with the use of synchrotron radiation (SR) has a unique combination of spatial resolution and elemental sensitivity. This is a recent and rapidly evolving technique, which benefited from its implementation in new, third generation, synchrotron storage rings such as the APS in Argonne, IL or the ESRF at Grenoble, France [12,13]. These new synchrotrons have a much higher brightness than previous ones, and thus allow to acquire fluorescence spectra with <ppm sensitivity in a matter of minutes.

Experimental approach:

In our attempt to determine the concentration of alloying elements in solid-solution, we adopted the following approach. The alloys studied here are composed of an α-Zr matrix containing minute amounts of transition elements in solid-solution and of second phase particles rich in these transition elements (Fig. 1). Most second-phase particles found in Zircaloy-4 recrystallized are of the types $Zr(Fe, Cr)_2$ or $Zr_2(Fe,Cr)$ [14,15]. The second-phase particles in ZIRLO are of ZrNb and ZrNbFe types. A study of second phase particles in Zircaloy-4 and ZIRLO using the Advanced Photon Source is presented by the authors in the proceedings of ICONE 8 [16]. In order to sample the concentration of elements in matrix only, we have to be able to "see" the second phase precipitates and control the relative positions of the beam and the sample to depart from them. The difficulty that arises is that the relative positioning of the beam with regard to the sample at a microscopic length scale has to be done "blind". In effect, the beam is not visible and so, an optical device such as a CCD or a microscope does not help. The method we used consists of rastering the sample in the beam with the help of a precision scanning stage and recording the fluorescence intensity from transitions corresponding to elements found in precipitates, such as Fe or Cr. The energy dispersive detector at the 2-ID-D/E beamline at APS records a fluorescence spectrum into up to 4048 digital channels. The scanning software allows to define up to 10 spectral "regions of interest" from this spectrum, and to record them simultaneously vs. the specimen position during a 2D scan. By choosing these ROI's to coincide with fluorescence lines of the elements of interest, the 2D distribution of these elements can be mapped. As the concentrations in Fe and Cr are much higher in the precipitates than in the matrix, the precipitates appear as brighter regions in the intensity maps for these elements (more intense fluoresced signal). The stage then allows to set the beam on the matrix region. Once the x-ray beam is positioned on the matrix, we can acquire a fluorescence spectrum over the whole range of energies below the incident beam energy.

Some conditions have to be fulfilled for this method to be applicable. The relative sizes of the beam, the precipitates and the distance between precipitates determine the possibility to differentiate the precipitates from the matrix in intensity maps. For example, if the beam is much wider than a particle, the intensity from this particle is averaged with that from the surrounding matrix and its image in the resulting 2D scan gets smeared out, producing a "blurred" image of the sample. Similarly, if the beam is larger than the distance between two precipitates, fluorescence counts from those are counted at any position in between them, raising the matrix intensity and blurring the map. For this last case, it is also to be noted that x-rays at the energies used here can penetrate the alloys on distances that are large compared to the expected average inter-precipitate distance, which is about 1 μm for a precipitate number density of 10^{12} cm^{-3}.(typical of the density found in Zircaloy-4) The absorption distances of x-rays by Zr and Sn - the major elements in our samples- are given for some energies of interest in table 2. An estimation of the probability to avoid hitting a precipitate with the incident beam is presented below.

Considering a beam of cross-sectional area A impinging on a sample of thickness w containing N precipitates per unit volume, the probability P_0 of avoiding hitting any particle is given by:

$$P_0 = e^{-N \cdot A \cdot w}$$

The precipitate number density N and beam size A have to be estimated. In previous experiments at the 2-ID-D/E beamline, a beamsize of 0.5 μm by 0.8 μm has been achieved. The number density N can be calculated easily if it is assumed that the amount of alloying elements in solid-solution is negligible compared to the amount in precipitates, and if the

	Zr (μm)	Sn (μm)
incident beam 9.2 keV	16.98	8.09
Fe Kα 6.4 keV	6.30	3.08
Fe Kβ 7.1 kev	8.20	3.97
Cr Kα 5.4 keV	4.00	2.00
Cr Kβ 5.9 keV	5.16	2.55

note: attenuation length =length after which intensity is decreased by a factor 1/e.

Table 2 Attenuation length of x-rays in pure elements.

particles are taken to be spherical. In effect, the total amount of alloying element is known and the average diameter of particles is experimentally related to the annealing parameter [15]. In Zircaloy-4 recrystallized, this diameter is approximately 200 nm, which gives a number density of precipitates $N=10^{12}$ cm^{-3}. For a specimen thickness of 10 μm, which is typical of dimpled samples, we then have $P_0=0.18$. We see that for this type of sample the probability to sample the matrix only is rather slim. As P_0 increases when w decreases, a way to overcome this problem is to use thinner specimens. For a thickness of 1000 Å and a particle density $N\approx10^{12}$ cm^{-3}, we have $P_0=0.96$. From the previous discussion, it appears that the thickness of the specimen is important to distinguish second phase particles from the matrix in 2D scans. TEM specimens usually are thinner than 1000 Å around the hole and thus present a larger space between particles, giving access to the matrix. Also, they are thin enough to avoid having precipitates located deep below their surface. Thus, they are ideally suited for this experiment. Besides they can be used and characterized in parallel in the TEM.

Another concern is that of the relationship between the fluorescence intensity recorded and the concentration of the elements. We use standard specimens to relate concentrations to intensities. The composition of these standards has to be known and should be homogeneous throughout the specimen. The shape of the standard also has to be as close as possible to that of the sample to be analyzed, in order to minimize the effects of geometry. The solution we adopted is to prepare TEM specimens out of annealed and quenched strips of the alloys. These quenched specimens show a homogeneous distribution of alloying elements equal to overall alloy concentration.

Specimen preparation:

The alloys studied were received in different shapes. We used plates of Zircaloy-4 (Z4) recrystallized and tubes of ZIRLO (ZL) recrystallized for 2 hours at 575ºC under Ar atmosphere. These tubes are sections of unirradiated cladding

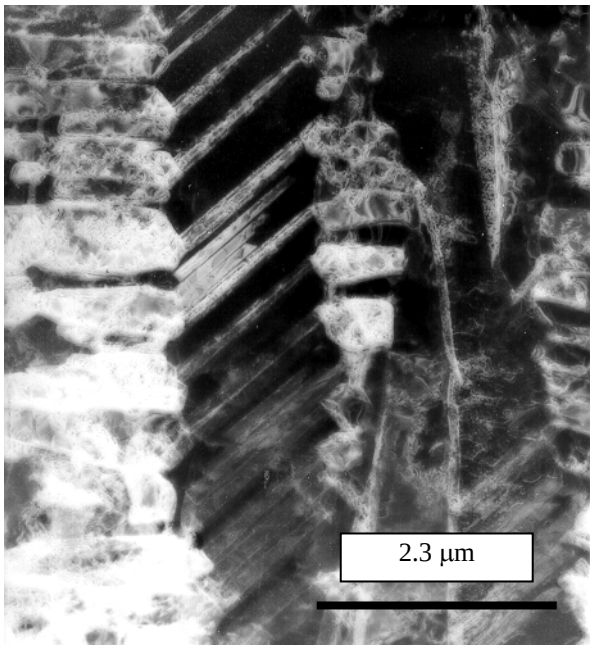

Fig. 2: Bright Field TEM micrograph of quenched Zircaloy-4.

tubes provided by Westinghouse. The Z4 plates are about 0.8 mm thick; the ZL tubes are 10.8 mm in diameter and have a wall thickness of 0.65 mm. We cut strips about 0.5 cm × 1 cm out of these alloys using a South Bay Technology low speed diamond saw. We ground them down to about 200 μm thickness using a mechanical grinder and 35 μm SiC grit paper.

Some dimpled samples were prepared for a trial run and in order to check our calculations. Those were first mechanically ground to below 100 μm thickness using 35 μm followed by 18 μm SiC grits. They were dimpled with a dimpler model D500i from VCR group, starting with 3 μm followed by 1 μm diamond grinding pastes, down to 5 μm thickness. From optical microscope examination, these samples are believed to thinner than 10 μm at their thinnest point.

TEM specimens were also prepared. For these samples, 3 mm discs were drilled from thinned strips. The specimens were prepared from these discs by a twin-jet electropolishing technique using a HCl, ethanol, 2-butoxyethanol solution. TEM examinations were conducted on the Philips CM 30 at ANL-Materials Science Division.

Quench procedure:

In order to obtain an homogeneous distribution of elements in the standards we dissolve the precipitates by carrying a β-phase anneal followed by a water quench that freezes the microstructure. We anneal Z4 and ZL strips for 10 minutes at 1000ºC under 0.5 atm. Ar in quartz tubes. The tubes are then broken in water for quench and TEM specimens are prepared from resulting strips. The TEM micrograph of Fig. 2 shows a low magnification view of a quenched Zircaloy-4 sample. The

martensitic structure of the grains resulting from the quench can clearly be seen. No precipitates are observable, as expected, and none were detected by chemical analysis of grain boundaries.

2 RESULTS

Figure 3 shows a TEM EDS spectrum (plotted in logarithmic scale) taken from the matrix of recrystallized Zircaloy-4 with the Philips CM 30 TEM at ANL-Materials Science Division. The measurement spot is shown by the pointer on the micrograph of Fig. 4. None of the transition elements Fe or Cr can be observed on the spectrum; the peaks corresponding to these elements are drowned in the background. Their concentrations in the Zr matrix are too low to be measured with this technique.

Figures 5 and 6 show intensity maps for the Fe Kα line that were recorded on a Z4 dimpled specimen and a Z4 TEM specimen respectively. The intensity plotted on these graphs is in units of relative intensity with respect to the lowest point. It is very clear how thinner specimens like TEM samples increase the contrast between the precipitates and the matrix. On the dimpled sample map, the maximum precipitate-matrix ratio of intensity is about 3.5, whereas on the TEM sample map, it is on the order of 80. This much better contrast allows for a clearer location of the precipitates in the matrix. The gaussian shape of the intensity peaks associated with the precipitates as well as their width -larger than the average precipitate size- suggest that the x-ray beam is larger than the particles and thus does not optically resolve them. The resulting gaussian shape is the effect of the convolution of the beam intensity profile with the elemental distribution profile of the precipitate. There are image reconstruction techniques to deconvolve such images and get the actual element distribution, provided the scanning step size is finer than half the size of the point-spread function (the size of the beam in our case) [17]. The maximum relative intensity of the precipitate peaks compared to the matrix is also lower than the expected concentration ratio between precipitate and matrix, even when using a TEM specimen. If one considers the solubility limit for Fe in the matrix to be about 50 at ppm for Fe, as discussed previously, and a concentration of Fe in the precipitates near 66% at., there is a ratio of 10,000 in the concentrations. It is likely that broadening of the precipitates due to the beam size (as well as other effects) could produce this difference between the concentration and the intensity ratios. The image we get from TEM specimens is still clear enough to locate precipitates accurately and sample the matrix only.

Figure 7 shows an x-ray fluorescence spectrum acquired in the APS from the matrix of the Zircaloy-4 annealed, at the point S indicated in the previous 2D scan. This spectrum very clearly shows the peaks associated with the alloying elements: Fe Kα, Fe Kβ, Cr Kα, Cr Kβ, as well as Cu Kα and the L lines of Sn. There is an additional strong peak from Ar Kα transition as the experiment is done in air. The elastic peak corresponds to incident x-rays that are elastically scattered in the sample. This peak allows to check the incident x-rays energy (9.2 keV). It is to be noted that the two spectra of Fig. 3 and Fig. 7 have been

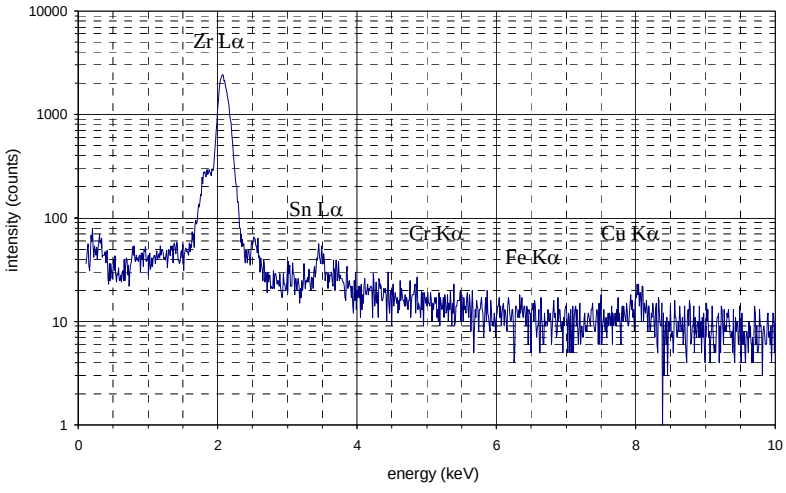

Fig. 3: EDS spectrum from the matrix of recrystallized Zircaloy-4.

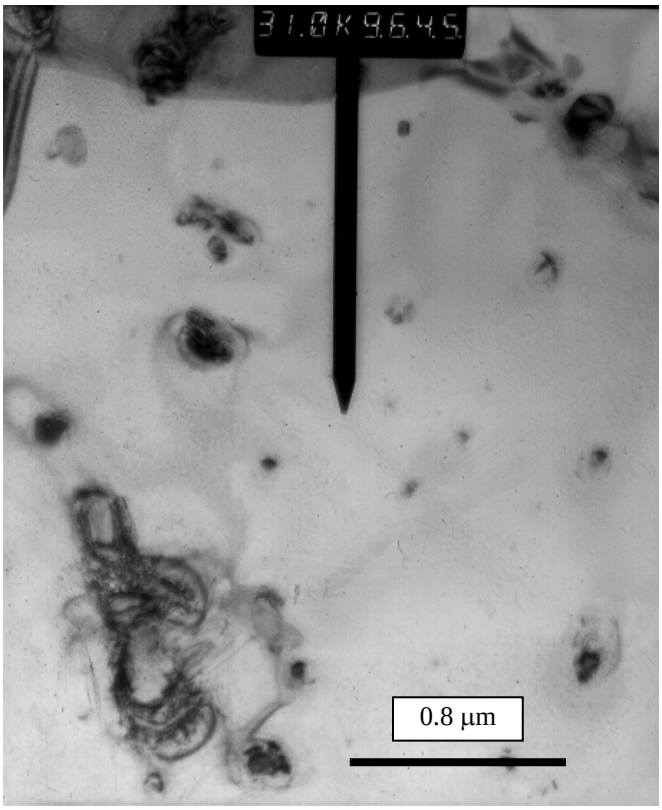

Fig. 4: Bright Field TEM micrograph from Zircaloy-4 (showing EDS spectrum

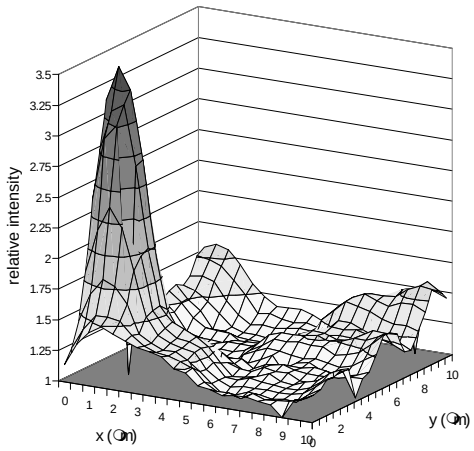

Fig.: 5 Fe Kα intensity map in recrystallized Zircaloy-4 dimpled specimen.

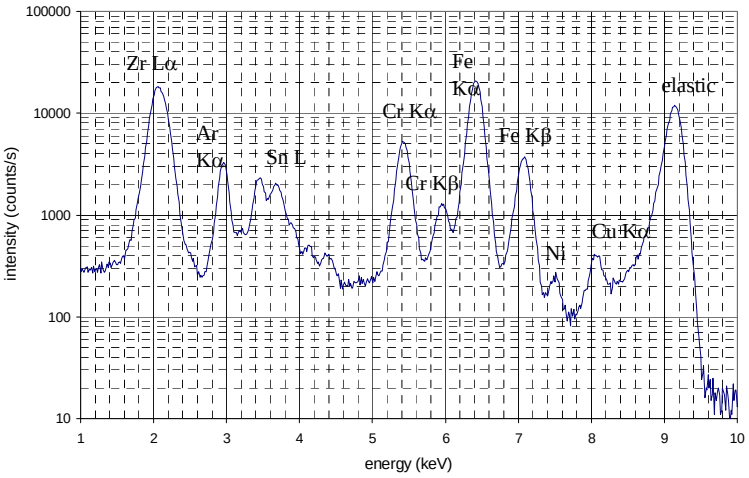

Fig. 7: X-ray fluorescence spectrum from the matrix of annealed Zircaloy-4 using the APS. Spectrum acquired at point S of map shown in Fig.6.

acquired over comparable measurement times: 300 s for the one from APS and about one minute for the TEM EDS one. Comparing the two figures, it is clear how much more sensitive the APS is in detecting the trace element concentrations.

Another method was also used to compare the concentrations of elements in a sample or in different samples. By scanning the sample along one direction and recording the fluoresced intensity, one gets an intensity profile, or 1D scan, that is related to the concentration profile in the sample. This method is quicker since it does not acquire data over as many points as a 2D scan. Figures 8 and 9 show such intensity profiles acquired on ZIRLO quenched and Zircaloy-4, respectively. As a first order approximation, it is assumed that both samples have the same shape and same thickness, which is reasonable as they were prepared in the same conditions. Around the central hole, TEM specimens are wedge-shaped; it is assumed that the slopes on both samples are the same, or close, for the same reason. By a linear approximation of the intensity curves, one finds an intensity slope for Fe in ZIRLO of 6670 cts/mm and of 1810 cts/mm for Fe in Zircaloy-4. By directly relating the ratio of these slopes to ratios of concentrations in the samples and given the Fe concentration in ZIRLO quenched of table 1 (0.11% weight), one finds a concentration of Fe in the Zircaloy-4 matrix of 300 wt. ppm. In order to evaluate the accuracy of this method, one can compare the ratio of the intensity slopes on 1D scans for Zircaloy-4 quenched and ZIRLO quenched to the ratio of the

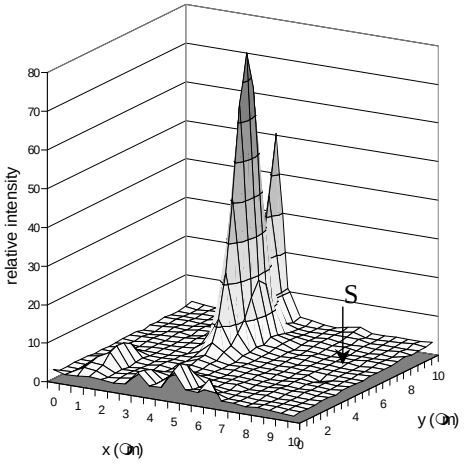

Fig. 6: Fe Kα intensity map in annealed Zircaloy-4 TEM specimen.

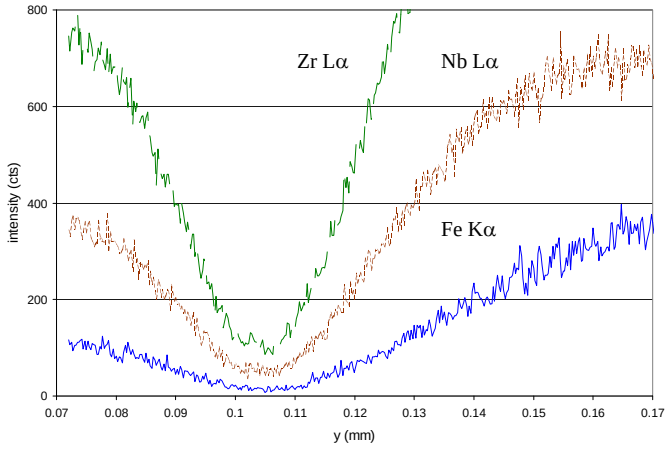

Fig. 8: Fluorescence intensity profile around the hole in a TEM specimen of quenched ZIRLO.

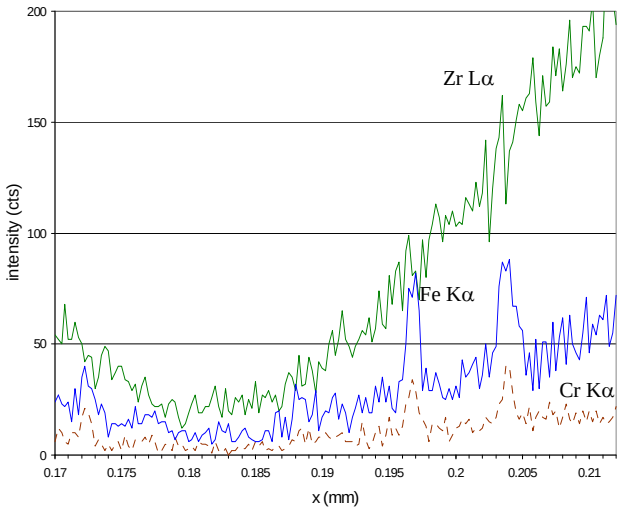

Fig. 9: Fluorescence intensity profile in Zircaloy-4 irradiated to 5 dpa with 1.5 MeV Kr+ ions at 575 K.

corresponding concentrations. The Z4/ZL ratio of linearized intensities for Fe is equal to 1.6. For comparison, the measured ratio of Fe concentrations in the two alloys is 2.2 (table 1).

3 DISCUSSION

The most important point in the experimental approach we discussed in the previous section is that of the relative positioning of the beam with respect to the precipitates embedded in the Zr matrix. In effect, we have to have avoid hitting precipitates in order to measure the alloying element concentration in the Zr matrix. If there is some intensity detected from a buried precipitate when we try to sample the concentration in the matrix, the alloying element peaks recorded are actually artifacts. This could happen if some precipitates are not revealed in the intensity maps and the matrix concentration is sampled in an area that is not truly precipitate-free. Thus, the precipitate/matrix intensity ratio-or "contrast"- in the 2D scans is of importance, as it allows to reveal discrete second phase particles. It is thought TEM samples allow a contrast high enough to avoid this problem. The attenuation lengths in Zr of the transition radiations of interest being much bigger than the thickness of TEM samples, it is improbable that a precipitate is not revealed by a 2D scan. The x-ray fluorescence spectrum from the matrix of Zircaloy-4 shown in Fig 7. was taken in a very flat area, of intensity much lower than that of the precipitate, which supports the hypothesis that it truly represents the matrix concentration. Besides, several spectra have been acquired on the matrix of Zircaloy-4 and they show comparable peak intensities for alloying elements. Another observation supports the statement that most of second phase particles are seen on intensity maps: the density of precipitates observed on these maps corresponds to that observed on TEM micrographs. The slope ratio method discussed at the end of the last section gives an estimation of the concentration of Fe in the matrix of Zircaloy-4. The precision of the linear slope fitting can be estimated to ±10%, so the comparison of slopes to real concentrations in quenched alloys indicates the accuracy of this method. It is about 30%. Finally, we note that the results we presented in this paper are preliminary, and a more in-depth quantitative analysis is currently under way.

4 CONCLUSION

This paper demonstrates that the measurement of very low concentrations of alloying elements in the Zr matrix of Zircaloy-4 and ZIRLO is possible using the 2-ID-D/E μ-XRF beamline at APS. This technique proves to be much more sensitive than TEM EDS to the very low concentration levels found in the alloys studied and the fluorescence peaks corresponding to the alloying elements of interest were very clearly observed. The use of TEM specimens for this experiment was necessary in order to discriminate the precipitates from the matrix and avoid artifacts. A preliminary estimate of the concentration in the matrix of Zircaloy-4 was also obtained.

ACKNOWLEDGMENTS

Thanks are due to R. B. Adamson at G.E. Vallecitos, and R. J. Comstock at Westinghouse Science and Technology Center for furnishing the samples used in this study. A. T. Motta would like to acknowledge helpful discussions with R. J. Comstock. We also wish to thank B. Kestel at ANL MSD for his expert preparation of TEM samples. This research was sponsored by the Department of Energy, Nuclear Engineering Education and Research (DOE-NEER) program, under grant number DE-FG07-98ID 13637. Use of the Advanced Photon Source was supported by the U.S. Department of Energy, Basic Energy Sciences, Office of Science, under Contract No. W-31-109-Eng-38.

REFERENCES

1. C. Lemaignan and A. T. Motta, "Zirconium Alloys in Nuclear Applications", *Nuclear Materials*, vol. 10 B, B.R.T. Frost ed., VCH New York, 1994, 1-51.

2. R. Borrelly, P. Merle and L. Adami, "Study of the solubility of iron in zirconium by thermoelectric power measurement", *J. Nucl. Mater.*, 1990, **170**, 147.

3. H. Zou, G. M. Hood, J. A. Roy, R. J. Schultz and J. A. Jackman, "The solid solubility of Fe in α-Zr: a secondary ion mass spectrometry study", *J. Nucl. Mater.*, 1994, **210**, 239.

4. D. Charquet, R. Hahn, E. Ortlieb, J-P. Gros and J-F. Wadier, "Solubility limits and formation of intermetallic precipitates in ZrSnFeCr alloys", *ASTM STP*, 1988, **1023**, 405.

5. **IAEA**, "Corrosion of Zirconium Alloys in Nuclear Power Plants", *IAEA*, Vienna IAEA-TECDOC-**684**, 1993.

6. A.T.Motta and C. Lemaignan, "A ballistic mixing model for the amorphization of precipitates in Zircaloy under neutron irradiation", *J. Nucl. Mater.*, 1992, **195**, 277.

7. H. Zou, G.M. Hood, J.A. Roy, R.H. Packwood, "Irradiation-driven solute redistribution in Zr alloys", *J. Nucl. Mater.*, 1997, **245**, 248-252.

8. G. M. Hood and R. J. Schultz, "Diffusion of 3D Transition Elements in α-Zr and Zirconium Alloys", *ASTM STP* **1023**, L. F. P. Van Swam and C. M. Eucken, Eds., American Society for Testing Materials, Philadelphia, 1989, pp. 435-450.

9. Y. De Carlan, C. Regnard, M. Griffiths, D. Gilbon and C. Lemaignan, "Influence of Iron in the Nucleation of <c> Component Dislocation loops in Irradiated Zircaloy-4", *11th Int. Symp. on Zr in the Nuclear Industry*, E. R. Bradley and G. P. Sabol eds., *ASTM STP* 1295, 638-653.

10. D. Pêcheur ; F. Lefebvre, A. T. Motta, C. Lemaignan and D. Charquet, "Oxidation of intermetallic Precipitates in Zircaloy-4 : Impact of Irradiation", *10th Int. Symp. on Zr in the Nuclear Industry*, A. M. Garde and E. R. Bradley eds., *ASTM STP* 1245, 1994, 687-708.

11. D. Pêcheur, F. Lefebvre, A. T. Motta, C. Lemaignan and J-F. Wadier, "Precipitate Evolution in the Zircaloy-4 oxyde layer", *J. Nucl. Mater.* **189**, 1992, 318-332.

12. F. Adams, K. Janssens and A. Snigirev, "Microscopic x-ray fluorescence analysis and related methods with laboratory and synchrotron radiation sources", *J. Anal. Atom. Spectrom.*, 1998, **13**, 330.

13. Z. W. Chen and D. B. Wittry, "Microanalysis by monochromatic microprobe x-ray fluorescence-physical basis, properties, and future prospects", *J. Appl. Phys.*, 1998, **84**, 1064.

14. E. A. Preble and K. L Murty., "A Review of Intermetallic Precipitates and Their Influence on Zircaloy Corrosion in Nuclear Reactors", *CORCON-97 Corrosion and Its Control. II*; Elsevier Science BV, 1998, 609-614.

15. P. Chemelle, D. B. Knorr, J. B. Van Der Sande and R. M. Pelloux, "Morphology and composition of second phase particles in Zircaloy 2", *J. Nucl. Mater.*, 1983, **113**, 58.

16. K. T. Erwin, O. Delaire, A. T. Motta, R. C. Birtcher, Y. Chu and D. Mancini, "Study of second phase particles in Zr alloys using the Advanced Photon Source at Argonne National Laboratory", these proceedings.

17. A. Lida, M. Takahashi, K. Sakurai and Y. Gohshi, "SR x-ray fluorescence imaging by image reconstruction technique", *Rev. Sci. Instrum.*,1989, **60 (7)**, 2458.

18. R. Jenkins, R. W. Gould and Dale Gedcke, "Quantitative X-ray spectrometry", Practical Spectroscopy Series, E. G. Brame Jr., M. Dekker, 1995.

19. G. R. Lachance and F. Claisse, "Quantitative X-ray Fluorescence Analysis : Theory and Applications", John Wiley, New York, 1995.

20. R. Tertian and F. Claisse, "Principles of Quantitative X-ray Fluorescence Analysis", Heyden & Son, 1982.